



A combined LC-MS and NMR approach to reveal metabolic changes in the hemolymph of honeybees infected by the gut parasite *Nosema ceranae*

Cyril C. Jousse, Céline Dalle, Angélique Abila, Mounir Traïkia, Marie Diogon, Bernard Lyan, Hicham El Alaoui, Cyril Vidau, Frédéric Delbac

► To cite this version:

Cyril C. Jousse, Céline Dalle, Angélique Abila, Mounir Traïkia, Marie Diogon, et al.. A combined LC-MS and NMR approach to reveal metabolic changes in the hemolymph of honeybees infected by the gut parasite *Nosema ceranae*. *Journal of Invertebrate Pathology*, 2020, 176, pp.107478. 10.1016/j.jip.2020.107478 . hal-03132817

HAL Id: hal-03132817

<https://uca.hal.science/hal-03132817>

Submitted on 17 Oct 2022

HAL is a multi-disciplinary open access archive for the deposit and dissemination of scientific research documents, whether they are published or not. The documents may come from teaching and research institutions in France or abroad, or from public or private research centers.

L'archive ouverte pluridisciplinaire **HAL**, est destinée au dépôt et à la diffusion de documents scientifiques de niveau recherche, publiés ou non, émanant des établissements d'enseignement et de recherche français ou étrangers, des laboratoires publics ou privés.



Distributed under a Creative Commons Attribution - NonCommercial 4.0 International License

Title

A combined LC-MS and NMR approach to reveal metabolic changes in the hemolymph of honeybees infected by the gut parasite *Nosema ceranae*

Authors : Cyril Jousse^{2,3*}, Céline Dalle^{2,3}, Angélique Abila^{2,3}, Mounir Traikia^{2,3}, Marie Diogon¹, Bernard Lyan^{2,3}, Hicham El Alaoui¹, Cyril Vidau⁴, Frédéric Delbac¹

¹ Université Clermont Auvergne, CNRS, Laboratoire "Microorganismes : Génome et Environnement", F-63000 Clermont–Ferrand, France.

² Université Clermont Auvergne, CNRS, Sigma-Clermont, Institut de Chimie de Clermont-Ferrand, F-63000, Clermont-Ferrand, France.

³ Plateforme d'Exploration du Métabolisme, Université Clermont Auvergne & I.N.R.A site de Theix, Clermont-Ferrand, France.

⁴ ITSAP, UMT PrADE, Inra – Acta, 228 route de l'aérodrome, F-84000, Avignon, France (current address).

* Corresponding author.

Email: cyril.jousse@uca.fr; Address: Institute of Chemistry of Clermont-Ferrand, 24 avenue Blaise Pascal, 63178 Aubière cedex, France

Highlights

* Honeybee hemolymph metabolome is altered by the gut parasite *Nosema ceranae*

* 15 metabolites were identified by LC-MS and NMR as candidate biomarkers of infection

* Putative biomarkers are involved in carbohydrate, amino acid and lipid metabolic pathways

25

26 **Abstract**

27 *Nosema ceranae* is an emerging and invasive gut pathogen in *Apis mellifera* and is
28 considered as a factor contributing to the decline of honeybee populations. Here, we used a
29 combined LC-MS and NMR approach to reveal the metabolomics changes in the hemolymph
30 of honeybees infected by this obligate intracellular parasite. For metabolic profiling,
31 hemolymph samples were collected from both uninfected and *N. ceranae*-infected bees at
32 two time points, 2 days and 10 days after the experimental infection of emergent bees.
33 Hemolymph samples were individually analyzed by LC-MS, whereas each NMR spectrum was
34 obtained from a pool of three hemolymphs. Multivariate statistical PLS-DA models clearly
35 showed that the age of bees was the parameter with the strongest effect on the metabolite
36 profiles. Interestingly, a total of 15 biomarkers were accurately identified and were assigned
37 as candidate biomarkers representative of infection alone or combined effect of age and
38 infection. These biomarkers included carbohydrates (α/β glucose, α/β fructose and
39 hexosamine), amino acids (histidine and proline), dipeptides (Glu-Thr, Cys-Cys and γ -Glu-
40 Leu/Ile), metabolites involved in lipid metabolism (choline, glycerophosphocholine and O-
41 phosphorylethanolamine) and a polyamine compound (spermidine). Our study
42 demonstrated that this untargeted metabolomics-based approach may be useful for a better
43 understanding of pathophysiological mechanisms of the honeybee infection by *N. ceranae*.

44 **Keywords:** Honeybee; Metabolomic; *Nosema ceranae*; Stress Biomarkers

45

46

47 **1. Introduction**

Honeybees provide essential ecosystem services in agricultural and natural areas by pollinating many crops and native plants. However, these insect pollinators are exposed to multiple abiotic (pollutants, pesticides) and biotic (infectious agents, parasites) stressors which are detrimental to their health and lifespan. Among them, both parasites and pesticides seem to be the most important stressors affecting honeybees and contribute to the decline of their populations (Goulson et al., 2015; vanEngelsdorp et al., 2009; vanEngelsdorp and Meixner, 2010).

The gut parasite *Nosema ceranae* is among the most common pathogens in *Apis mellifera*, with a worldwide distribution (Goulson et al., 2015) and is now considered to be a major threat to the Western honeybee at both the individual and colony levels (Fries, 2010; Higes et al., 2013; Paris et al., 2018; vanEngelsdorp and Meixner, 2010). Similar to other microsporidian species, *N. ceranae* can alter the bee physiology and behavior in order to maintain a more favorable environment for its reproduction. Several studies have demonstrated that *N. ceranae* infection impairs tissue integrity in the midgut (Dussaubat et al., 2012), alters the energy demand in honey bees (Alaux et al., 2009; Martín-Hernández et al., 2011; Mayack and Naug, 2009; Naug and Gibbs, 2009) and decreases hemolymph sugar level (Mayack and Naug, 2010). The infection also significantly suppresses the bee immune response (Alaux et al., 2009; Antúnez et al., 2009; Aufauvre et al., 2014; Chaimanee et al., 2012; Dussaubat et al., 2012) and alters pheromone production in worker and queen honey bees (Alaux et al., 2011; Dussaubat et al., 2010; Holt et al., 2013). Some studies also revealed that *N. ceranae*-infected honeybees have shorter lifespans than uninfected honeybees (Alaux et al., 2009; Goblirsch et al., 2013; Higes et al., 2006; Vidau et al., 2011). However, the presence of *N. ceranae* is not systematically associated with honeybee weakening and

mortality (Cox-Foster et al., 2007; Gisder et al., 2010; Invernizzi et al., 2009), suggesting modulations in the parasite virulence. Possible explanations for this variation include parasite or host genetics (Chaimanee et al., 2010; Dussaubat et al., 2013; Medici et al., 2012; Williams et al., 2008), climate (Chen et al., 2012; Gisder et al., 2010), nutrition (Alaux et al., 2010b; Fleming et al., 2015), or interactions with other stressors such as environmental contaminants or other parasites. Indeed, some recent studies demonstrated that *N. ceranae* can sensitize the honeybees to chemical stressors (Alaux et al., 2010a; Aufauvre et al., 2014, 2012; Pettis et al., 2012; Retschnig et al., 2014; Vidau et al., 2011; Wu et al., 2012).

In order to explain disorders and detect (early) modifications on bee physiology, we must acquire molecular tools to screen from genome to metabolome (Lankadurai et al., 2013). Among these tools, metabolomics is the most informative, looking at the end of the “omic cascade” for the small metabolites, and strongly linked to the phenotype (Alonso et al., 2015; Bundy et al., 2008; Fiehn, 2002; Liu and Locasale, 2017). Most of the time, to visualize a wide range of metabolites, several analytical techniques are required. Mass spectrometry (MS) is one of the most sensitive and precise technique, depending on mass spectrometer accuracy, but is limited by chromatographic coupling and in-source ionization. Nuclear magnetic resonance (NMR) spectroscopy provides the widest coverage of all techniques. Nevertheless, sensitivity and resolution are regular drawbacks.

Untargeted metabolomics has the advantage to highlight both known and unknown metabolites resulting from phenotypic evolution. Based on statistical filters, all signals from analytical devices (MS and/or NMR) are examined for possible correlation with the observed biological effect (Wishart et al., 2008). Those with high correlation will be submitted to deeper analyses as data/base mining, MS-MS and/or 2-dimensional NMR experiments if needed, to reveal the identity of the associated biomarker.

One of the most established protocols in metabolomics is the metabolic profiling of plasma (Simón-Manso et al., 2013; Zhao et al., 2010) and urine (Zhang et al., 2012) on “higher animals”. Biological fluids are easy to collect and store and contain a wide range of metabolites that can be impacted by many physiological disturbances including medication, nutrition or disease (Zhang et al., 2020). In this way, researchers aim to find host biomarkers for early diagnosis of infectious diseases, collect evidence of metabolic disorders along time-periods or improve nutrition benefits. Hemolymph is the sole biofluid in the insect, analogous to the blood in invertebrates, and is composed of fluid plasma in which hemolymph cells (hemocytes) are suspended. It circulates in the interior of the insect body and remains in direct contact with the animal's tissues. Analyzing this fluid is an opportunity to access to metabolic pool impacted by stressors (Aliferis et al., 2012; Wang et al., 2019). Aliferis et al. (2012) previously reported by GC/MS the metabolite profiling of hemolymph in bees naturally infected by *N. ceranae*. They revealed that a gut parasite can induce a general disturbance of the honeybee physiology.

In our study, we have developed a methodology to perform metabolomics on hemolymph samples, using combined LC/MS and NMR approaches. The aim was to investigate the metabolic response of honeybees following experimental infection of emergent bees by *N. ceranae*. Metabolome of the hemolymph was examined in both infected and uninfected honeybees at two post-infection times.

2. Materials and methods

2.1. Biological experiments

2.1.1. Honeybee artificial rearing

All experiments were performed with a mixture of honeybees taken from three Buckfast colonies of the same apiary at the Laboratoire Microorganismes : Génome et Environnement (UMR 6023, Université Clermont Auvergne, France). We confirmed that the three colonies were free of *Nosema* (sampling of 30 foragers for each colony) by PCR using specific primers as previously described (Higes et al., 2006). Two frames of sealed brood were placed in an incubator in the dark at 33°C with 60% relative humidity. Emerging honeybees (100 per colony) were collected, confined to laboratory Pain-type cages in two groups (infected vs uninfected, see below for the infection procedure) of 50 individuals, and maintained in the incubator. During this time, honeybees were fed *ad libitum* with candy (Apifonda®) supplemented with fresh pollen (Naturapi). In order to mimic the colony environment, a small piece of wax and a 5-mm piece of Beeboost® (Pherotech, Delta, BC, Canada) releasing five queen mandibular pheromones, were placed in each cage. Each day, feeders were replaced; dead bees were counted and removed.

2.1.2. Experimental infection with *Nosema ceranae*

Spores of *N. ceranae* were obtained from bees experimentally-infected in the laboratory and the infection process was conducted as previously described (Vidau et al., 2011). Briefly, the intestinal tract of infected bees was dissected and homogenized in PBS and the resulting suspension was filtered through Whatman No 1 filter paper, cleaned by centrifugation and resuspended in PBS. At 5 d post-emergence, caged honeybees were starved for 3 h, CO₂-anaesthetized and individually transferred in “infection boxes” consisting of 40 ventilated compartments (3.5 cm³). Each compartment was supplied with a tip containing 125,000 spores of *N. ceranae* diluted in 3 µL of water. “Infection boxes” were placed in the incubator

and 1 h later, bees that had consumed the total spore solution were again caged (50 bees per cage). Uninfected bees were similarly treated without *N. ceranae* spores in the water. At the end of the experiment, we checked that the control remained uninfected.

2.1.3. Hemolymph sampling

Hemolymph samples were collected at day 2 (D2) and day 10 (D10) post-inoculation from both infected and control (uninfected) honeybees using the method described by (Mayack and Naug, 2010). Bees were first CO₂-anaesthetized and placed on ice, before antenna cutting. Immediately, honeybees were placed into PCR tube and centrifuged at 16,000 x *g* during 30 s. Hemolymph was collected in a new tube and stored at -80°C until analysis.

2.2. Chemical analyses

2.2.1. Chemicals and reagents

Creatinine (Fluka), phenylalanine and tryptophan (Sigma-Aldrich) were used as external standards for LC/MS quality control. For NMR experiments, Deuterium oxide (D₂O) was purchased from Eurisotop and 3-(trimethylsilyl) propionic-2,2,3,3- tetra-d₄ acid sodium salt (TSP-d₄) was purchased from Sigma-Aldrich. Acetonitrile (Optima LC-MS), water (Optima LC-MS) and ammonium acetate (Optima) were purchased from Fisher Scientific for LC/MS analyses. MS external calibration was performed using lithium hydroxide monohydrate and formic acid (Fluka).

2.2.2. Standard solutions and sample preparations for LC/MS and NMR

Stock solutions were prepared for each standard compound (creatinine, phenylalanine and

tryptophan) at a concentration of 0.5 mg/ml in water/acetonitrile 1:1 containing 0.1% formic acid and were stored at -20°C. A mix of all standard solutions was extemporaneously prepared, for a final concentration of 5 µg/mL. Repeated analyses of the mixed standard solution ensure system stability before analysis of biological samples. Forty-eight hemolymph samples (10 µL each, 12 per modality) were diluted in water (LC/MS grade) 1:4 to decrease viscosity and provide a sufficient volume, considering LC sampling capabilities. Finally, 5 µL was injected in LC/MS for each analysis. For ¹H-NMR analyses, 51 hemolymph samples (12 bees per modality, but 15 for infected ones at D10) were centrifuged at 14000 x *g* for 10 min at 4°C. Three hemolymph samples (from the same experimental condition) were pooled (to reach the minimum volume required for NMR experiment) and the final volume was adjusted to 50 µl with D₂O. The Metabolic Profiler® platform robot (Bruker) prepared all analytical samples by mixing 50 µl of pooled samples with 150 µl of phosphate buffer (1.5 M phosphate in D₂O at pH 7.06). D₂O was used for shimming and locking, whereas TSP-d₄ constituted a reference for chemical shifts (0 ppm) for NMR. Finally, 180 µl of the solution was injected, through a capillary, for the online ¹H-NMR profiling. Quality control samples were also prepared using aliquots from each analytical sample. They ensure system stability and permit to improve spectra processing.

2.2.3. Metabolic profiler® platform (Bruker Biospin, France)

Ultraperformance liquid chromatography-mass spectrometry (UPLC-MS) used was a MicroToF system (Bruker) equipped with an electrospray ionization probe (ESI) and a 1200 series chromatographic system (Agilent). Chromatographic separation was performed with a kinetex HILIC column (100 x 2.1mm, 2.6 µm, Phenomenex) with pre-column. The mobile phase was composed with acetonitrile (A) and water (B) solvents, both containing 10 mM

ammonium acetate. The flow rate was 0.4 mL/min and the gradient elution was carried out as follows: 0-2 min at 100% A; 2-4 min linear gradient to 80% A; 4-13 min linear gradient to 20% A and back to 100% A into 10 sec (initial conditions); 1 min 50 sec equilibration wash with 100% A, for a total run of 15 min. The injection volumes for both samples and standards were 5 μ L and the column temperature was set at 25°C. Blanks of pure water and pure acetonitrile were injected after every 10 hemolymph samples, for cleaning the chromatographic system. The mass spectrometer was calibrated with lithium formate clusters (5 mM into water) and operated in positive ion mode for full scan (50-1000 m/z) detection. Nitrogen was used as the nebulizer and the drying gas. The nebulizer pressure was 2 bars, the desolvation gas flow rate was 8 L/min and desolvation temperature was maintained at 200°C. Capillary tension was 4000 V.

On flow 1-dimensional ^1H -NMR experiments were done on an Avance III 500 MHz NMR spectrometer, using an inflow 3-mm FISEI z-gradient (^1H - ^{13}C) probe with a 60- μ l cell. A standard one dimensional noe spectroscopy sequence (noesygppr1d with water presaturation and gradients) was used with low power irradiation of the water resonance during the recycle delay of 4 s and the mixing time of 10 ms. 256 scans were collected with an 90° impulsion time of 9.29 μ s, an acquisition time of 3.28 s, a spectral window of 10000 Hz and 64K data points zero-filled to 128K before Fourier transformation with 0.3 Hz line broadening. All NMR spectra were recorded at 300K and processed with Topspin version 2.1.

2.2.4. Ultrapformance liquid chromatography-tandem mass spectrometry (UPLC-MS-MS)

For identification purposes, a few samples from each condition, and that were representative for the features in the model, were analysed in full scan (80-1000 m/z) for positive ion mode on an LTQ Orbitrap Velos MS with same chromatographic conditions (gradient, column) as for

UPLC-MS profiling. The m/z of each feature was searched in the resulting chromatograms to obtain a better mass accuracy of the features, which was used to determine the most probable molecular formulae. The parent ion was identified from in-source fragments and adducts, and additional structural information on the features was obtained by performing MS/MS fragmentation on relevant ions using MS-MS in product ion scan mode with collision energies of 10, 20, and 30 eV. All information on the features was used to search into chemicals and metabolites databases (cf. § 2.5.3).

2.2.5. 1D and 2D NMR experiments for metabolite identification

For the metabolite identification step, the sample corresponded to a pool of 25 hemolymphs (mix of both infected and uninfected bees). The total volume of hemolymph (300 μ l) was mixed with 300 μ l of phosphate buffer in D_2O . The NMR spectrometer used (TGIR - CNRS de Gif/Yvette) was a Bruker Avance III 950 MHz equipped with a cryoprobe (1.7, 3 and 5 mm tube) TCI ($^1H/^{13}C/^{15}N/^2H$) with z-gradient coil probe (Bruker Biospin Wissenbourg, France). For 1D 1H -Spectra, a standard one dimensional noe spectroscopy sequence (noesygprr1d with water presaturation and gradients) was used with low power irradiation (31 μ W) of the water resonance during the recycle delay of 10 s and the mixing time of 10 ms. 128 scans were collected with a 90° impulsion time of 8.1 μ s, an acquisition time of 3.3 s, a spectral window of 10000 Hz and 64K data points zero-filled to 128K before Fourier transformation with 0.3 Hz line broadening. For 2D homonuclear (COSY TOCSY, JRES) and heteronuclear ($^1H/^{13}C$ HSQC and HMBC) experiments were performed with quadrature phase detection in dimensions, using state-TPPI or QF detection mode in the indirect one. For each 512 (80 for JRES) increments in the indirect dimension, 2K data points (8K for JRES) were collected and 16 transients were accumulated in the direct dimension. ^{13}C decoupling (GARP) was

performed during acquisition time for heteronuclear experiments. A $\pi/2$ shifted square sine-bell function was applied in the two dimensions before Fourier transformation. Spectra were treated with Topspin version 3.1. All NMR spectra were recorded at 300K.

2.3. Data management

2.3.1. Data extraction

MS data were converted into NetCDF format and extracted to data matrix using XCMS package under R environment (v. 2.15.3). Briefly, after ion extraction (m/z), a retention time (RT) correction was performed before production of the matrix including for each ion (m/z@RT) the relative intensity (area) detected into each analytical sample. Finally, CAMERA package (Kuhl et al., 2012) proposed a first annotation according to common adducts and natural isotopes. NMR data were binned using AMIX software (v. 3.9.10, Bruker) after alignment and baseline correction. Extraction process was chosen as follows: fixed bucketing of 0.01 ppm, from 0.13 to 10 ppm; solvent signal exclusion between 4.7 and 4.9 ppm; signals integration on the sum of intensities; normalization on total intensity. The resulting matrix was used for statistics.

2.3.2. Statistical analyses

Multivariate analyses were performed using SIMCA-P+ (v. 12.0.1.0, Umetrics) for non-supervised (PCA) and supervised ((O)PLS-DA) methods. Two normalization methods were tested, univariate (UV) and pareto (PAR), in order to obtain the most robust statistical models. All statistical models were validated according to explanatory (R^2) and predictive (Q^2) values as well as with random permutations. Lists of signals (ions or buckets) were

selected for each model according to VIP (variable importance in projection) scores (>1). For all valid models, a list of ions considered to be the most implicated was selected, according to VIP score. Univariate analyses were performed on Excel software (Windows) for ANOVA filtering on MS data. ANOVA multiway, with interaction, was performed in order to separate analytical effects from biological ones and to distinguish, when possible, age and infection metabolic effects.

2.3.3. Metabolite identification

Identification of VIP ions was performed manually or using R script for data mining on several public metabolic databases (KEGG, MetaCyc, HMDB). MS-MS fragmentation features were compared to MassFrontier (v. 7; ThermoScientific) theoretical schemes and databases (MassBank, METLIN, HMDB, PRIME). NMR VIP signals (buckets) were attributed manually using previously published data (Fan, 1996; Nicholson et al., 1995; Willker et al., 1996) and the human metabolome public database (HMDB).

3. Results

For metabolic profiling, hemolymph samples from both uninfected (UI) and *N. ceranae*-infected (I) bees were collected at two time points considered as early (D2) and late (D10) times of infection, respectively. Forty eight samples (12 for each modality) were individually analyzed by LC-MS in two batches (23 samples for batch 1 and 25 samples for batch 2). For ¹H-NMR experiments, hemolymph from 51 bees were pooled in 17 groups of three.

3.1. LC-MS profiles and metabolite identification

287 All hemolymph samples analyzed by LC-MS showed similar “total ion chromatogram”
288 profiles (**Suppl. Fig. 1**). Multivariate models were then applied to measure age (D2 vs D10)
289 and treatment (I vs UI) effects from a data matrix of 1294 ions. Among each analytical batch,
290 PLS-DA models clearly showed that the age of bees remained the parameter with the
291 strongest effect (**Figure 1**) and no statistical model was valid considering the infection effect
292 only. ANOVA filtering permitted discrimination between batch effect and combined effect of
293 age and infection, and all ions with a p-value above 0.05 were eliminated. A final list of 15
294 ions according to VIP scores, with levels significantly up- or down-regulated (at D2 and/or
295 D10), was then used for metabolite identification. Eight metabolites, corresponding to
296 potential biomarkers representative of infection alone or combined effect of age and
297 infection, were accurately identified according to spectral data and/or standard comparisons
298 (**Table 1**). These biomarkers included 3 dipeptides (Glu-Thr, Cys-Cys and γ -Glu-Leu/Ile), one
299 amino acid (histidine), one amino sugar (hexosamine), two metabolites involved in lipid
300 metabolism (glycerophosphocholine and O-Phosphorylethanolamine) and ethyl aconitate, a
301 tricarboxylic acid derivative, listed as flavoring agent. For each selected marker,
302 infected/uninfected (I/UI) ratios were mentioned at both D2 and D10 post-infection times.
303 The most interesting metabolite was hexosamine. In hemolymph of infected bees, the
304 circulating amount of hexosamine was 3x lower at D2 and 7-8x higher at D10 compared to
305 the control (**Table 1**). Similarly, in infected bees compared to control, levels of circulating
306 histidine and another “amino acid-like” putative compound were lower at D2 and higher at
307 D10. Three other metabolites (glycerophosphocholine and two dipeptides, Cys-Cys and Glu-
308 Thr) exhibited an opposite pattern. These circulating metabolites were more abundant at D2
309 and lower at D10. O-phosphorylethanolamine, a “sulfur-containing” putative metabolite and
310 peptides (γ -Glu-Leu/Ile and another putative “short peptide”) were detected at higher levels

in the hemolymph of infected bees at D2 and D10. Finally, ethyl aconitate, levels of circulating “carbohydrate-like” and “amine-like” putative compounds were lower in infected bees than in control bees, at the two time points post-infection.

3.2. NMR profiles and metabolite identification

Each NMR spectrum was obtained from a pool of hemolymphs from three honeybees. Spectra analysis showed signal richness of both aliphatic and sugar zones, below 5 ppm (**Suppl. Fig. 2**). Using multivariate statistical analysis tools, we observed a strong effect of ageing with PCA and PLS-DA models (**Figure 2**). Similar to MS results, age had the strongest effect and no valid model was obtained when considering the infection parameter alone. Buckets were selected according to VIP score (above 0.99). Eight biomarkers were clearly identified, according to spectral data and databases comparisons, and I/NI ratios were calculated at both D2 and D10 (**Table 2**). These biomarkers included four carbohydrates (fructose and glucose, both α and β forms), one amino acid (proline), a polyamine compound (spermidine) and two metabolites involved in lipid metabolism (choline and glycerophosphocholine). Signals for carbohydrates (fructose and glucose) shared similar behaviors. These compounds were more abundant in the hemolymph of infected bees particularly at the early infection time (D2). In contrast, proline was always less abundant in infected hemolymph. As for the MS data, levels of circulating glycerophosphocholine were higher in the hemolymph of infected bees at D2, then decreased at D10. Choline showed a completely opposite pattern. Although the amount of spermidine decreased at D2 for infected bees, no significant difference was observed at D10 between I and UI samples.

4. Discussion

335

336 **4.1. Biological sampling**

337 This proof of concept study was performed to develop transposable methodologies for
338 metabolic profiling on honeybee hemolymph from bees in hives and was linked to a study of
339 experimental infection of caged honeybees by the gut parasite *N. ceranae* conducted to
340 reveal metabolic shifts during the infectious process. We also raised several questions about
341 the quality and variability of biological samples.

342 Experimental results have suggested difficulties in assessing the health status of honeybees
343 from hives in field conditions. Both biotic and abiotic stressors may produce effects on the
344 physiology of the bees and modify the metabolic pool. Even using molecular biology (RNA
345 seq and/or qPCR) and analytical (multiresidue detection) tools, it is too time consuming and
346 costly to evaluate unstressed bees (*i.e.* healthy bees). Only visual symptoms and mortality
347 were evaluated during the experiment. In our opinion, difficulty in obtaining clear signatures
348 of *Nosema* infection in natural populations are partly due to honeybee genetic variability.
349 For example, Kurze et al. (2015) demonstrated that *Nosema*-tolerant honeybees were able
350 to escape the manipulation of apoptosis by the parasite. In addition, when a study follows
351 mortality across time, the major risk in sampling surviving bees is to artificially select
352 resistant insects with low-level infections or those less sensitive to infection (*e.g.* genetic
353 tendencies). However, even if honeybees are generally stressed by various factors, our study
354 should reveal the metabolic impact of the infection.

355 Finally, other limitations for biological sampling could be the drastic treatments for bee
356 infection, CO₂ anesthesia and hemolymph harvesting. In order to prevent any
357 artificial/technical disruptions, following a rigorous protocol is mandatory ("The

Metabolomics Standards Initiative (MSI) and Core Information for Metabolomics Reporting (CIMR),” n.d.).

4.2. Analytical experiments

Discriminating metabolic disturbances is an important issue in metabolomics. Firstly, metabolic coverage, in term of quality and quantity, is strongly linked to analytical tools. Mass spectrometry did not permit easy distinction of isobaric metabolites with similar fragmentation schemes. For this reason, based on our data, it was not possible to distinguish Ile/Leu containing compounds or reveal which hexosamine(s) is (are) impacted. Some NMR signals for ratio calculation were mixed in the same bucket and, thus, polluted. For that reason, they were discarded from our list (e.g. other fructose signals; data not shown). For these reasons, hyphenation using LC-MS, GC-MS and/or NMR is one of the best ways to harvest information, as precisely as possible (Wishart et al., 2008).

Secondly, with a very large amount of metabolic signals, data treatments and statistics are required to filter and reveal significant elements before any identification efforts (Monnerie et al., 2019). In our study, combining LC-MS and NMR metabolomics datasets improved coverage of the metabolome. Processing workflows (R packages; (Giacomoni et al., 2015) are time consuming but ensure data reproducibility and comparability. The differences in the metabolome profiles were deciphered using multivariate statistics (PLS-DA). Many statistical tools are able to manage such datasets, but multidimensional representations permit maintenance of data integrity and complexity. Such approach reveals, at the same time, the variability of the complete dataset and the group of signals that are most relevant considering the scientific hypothesis (Boccard and Rudaz, 2014). Analytical redundancy (e.g.

hexosamine in MS; Choline and spermidine in NMR) and metabolic interaction are keys for the explanation of such statistical effects and reinforce the identification of biomarkers. Finally, LC-MS-MS as well as 2D-NMR enhanced the identification of biomarkers. They are low throughput experiments, mostly targeted on the few signals of interest, but increase the quality of the identification. Data mining should be time consuming depending on what kind of metabolite is highlighted. The well-known primary metabolite is quickly identified; those less documented will take time to be identified with certainty. But guessing for “*de novo*” identification (no information in databases) requires high resolution analytical experiments to succeed.

4.3. Biomarkers of the infection and impacts on honeybee metabolism

Because hemolymph is the sole biofluid which circulates in the interior of arthropod body, we can infer that the metabolome of a hemolymph sample reflects the exchanges occurring between organs (digestive, neural, reproductive, etc.) during the infectious process. As expected, the age of bees was the parameter with the strongest effect on the hemolymph metabolome. However, we succeeded in identifying 15 metabolites that were assigned as candidate biomarkers representative of infection alone or the combined effect of age and infection. The levels of these metabolites could be interpreted as either a deleterious impact of infectious process or a defensive response against the pathogen.

The same pattern was observed for O-phosphorylethanolamine (PE), the dipeptide Glu-Leu/Ile, glucose and fructose (α and β forms). These metabolites were more abundant in the hemolymph of infected bees, particularly at D2 post-infection. Glycerophosphocholine (GPC; one major form of choline storage) identified by both LC-MS and NMR, as well as two other dipeptides (Cys-Cys and Glu-Thr), were also increased in infected samples but only at early

time of infection (D2). These observations could be related to impacts on proteins as building blocks and glycerophospholipid used in nervous and parasympathic systems. Infection is known to increase energetic demand and modify behavior in *N. ceranae*-infected bees (Alaux et al., 2010a; Martín-Hernández et al., 2011; Mayack and Naug, 2009; Naug and Gibbs, 2009). Some dipeptides also are known to have physiological or cell-signaling effects, although most are simply short-lived intermediates on their way to specific amino acid degradation pathways following further proteolysis. Some recent studies showed that lipid depletion is a phenomenon strongly linked to pathogen development (Franchet et al., 2019; Li et al., 2018). The level of amino acids and spermidine was lower in *Nosema*-exposed samples at D2 post-infection, whereas an antagonistic pattern occurred at D10 between proline and histidine. Decreased levels of amino acids, including proline, were also observed by (Aliferis et al., 2012) in the hemolymph of bees naturally infected by *N. ceranae*. Spermidine seems to be unmodified at D10. Proline and spermidine are involved in a key pathway, the arginine and proline pathway, at the boundary of important metabolisms (amino acids, glutathione, polyamine, etc.). Proline, the dipeptide Glu-Thr and GPC decreased at D10. The level of proline decreased as well in infected bees at D2 while the others increased. Hexosamine, the amino acid histidine and the amino alcohol choline showed a different pattern. The levels of these three metabolites were lower in infected bees at D2 and higher at D10 when compared to uninfected bees. Hexosamine may lead to the biosynthesis of chitin, one of the essential components of insect cuticle and peritrophic matrix in the gut. The peritrophic matrix lines the midgut of most insects and is a protective barrier against microbial infections (Kelkenberg et al., 2015). Chitin is also a major component of the cell wall of microsporidian spores (Bigliardi et al., 1996). Some studies revealed a degeneration of the peritrophic membrane in bees infected by *N. ceranae*

(Dussaubat et al., 2012). Thus, the higher level of hexosamine detected in the hemolymph of infected bees at D10 could be the result of degradation of the peritrophic matrix during the infectious process.

CONCLUSION

This study is the first presenting a complete methodology to analyze bee hemolymph using the up-to-date technologies for metabolomics, MS and NMR. The aim of our study was to detect signatures of the pathological processes during the infection of bees by the gut parasite *N. ceranae*. As a proof of concept, we identified biomarkers that could be useful for a better understanding of pathophysiological mechanisms of the honeybee infection by *N. ceranae*.

For further experiments, we recommend evaluation of the identified biomarkers, through precise quantification, on workers from hives under different field conditions. This untargeted metabolomic approach could also be used to identify biomarkers in the gut during the progression of the infection. In order to reduce disturbances related to other biotic or abiotic factors, we propose to use hives under insect mesh tunnels and follow health status of colonies through random testing.

Acknowledgement:

This work was funded by grants from the French National Research Agency (ANR, grant number ANR-12-BSV3-0020) and received support from PIA METABOHUB (ANR-AA-INSB-0010) and TGIR-RMN (IR-RMN-THC Fr3050 CNRS).

Figure captions

453

454 **Figure 1. PLS-DA on LC/MS profiles.** Batch 1 with 23 analyses (1), Batch 2 with 25 analyses
455 (2). Box for Day 2, dot for Day 10, blue figure for uninfected samples and red for infected
456 ones. A strong age effect is shown on the two batches (dashed black line). (1) PC1 (25,7%)
457 and PC2 (18,3%), (2) PC1 (20,9%) and PC2 (12,4%); Hotelling T2 (ellipse) = 95%.

458

459 **Figure 2. PLS-DA on NMR data.** Box for Day 2, dot for Day 10, blue figure for uninfected
460 samples and red for infected ones. An age effect is shown on the model (dashed black line).
461 PC1 (44,8%) and PC2 (14,1%); Hotelling T2 (ellipse) = 95%.

462

Table 1: Putative biomarkers identified from LC-MS and MS-MS experiments; ID was obtained from XCMS package (p for positive ionization; first number as mass on charge measurement; T for retention time; second number as the retention time of the ion in minutes). Infected/Uninfected (I/UI) ratios, at two time points (Day 2 and Day 10), were calculated on data matrix (relative intensities). Candidate names were proposed according to data obtained by LC-MS and MS-MS analyses and compared with databases and/or standards. ANOVA filtering distinguished between biomarkers linked to infection only (I) or to both infection and age (II). Signals were identified according to a mass precision less than 1 ppm, except for * 5 ppm far and ** 20 ppm far.

ID	I/UI @ D2	I/UI @ D10	Putative name	ANOVA
p133,058T6,3	0,14	1,55	Aminoacid like	I
p142,03T8,2	1,81	1,40	O-Phosphorylethanolamine	I
p179,054T6,4	0,45	0,63	Carbohydrate like	I
p203,059T5,7	0,42	0,86	Ethyl aconitate **	I
p246,249T5,8	0,84	0,36	Amine like	I
p251,044T6,3	1,17	3,40	Sulfur containing	I
p261,045T7,1	4,75	3,09	γ -Glu-Leu, γ -Glu-Ile	I
p399,134T8,2	2,84	1,67	Short (tri or tetra-) peptide	I
p145,052T5,6	0,36	8,57	Fragment of hexosamine	II
p156,078T8,7	0,52	1,18	Histidine	II
p180,093T5,6	0,38	6,64	Hexosamine	II
p181,092T5,6	0,34	7,26	¹³ C of hexosamine	II
p225,035T6,3	2,38	0,41	Cys-Cys *	II
p249,113T6,9	1,47	0,36	Glu-Thr	II
p280,102T8,3	1,21	0,45	Glycerophosphocholine	II

474

475 **Table 2: Putative metabolite biomarkers identified from NMR experiments;** ID was
 476 obtained with AMIX software (the center of each bucket), and Infected/Uninfected (I/UI)
 477 ratios, at the two time points (Day 2 and Day 10), were calculated on extracted matrix
 478 (relative intensities). Candidate names were proposed according to Identification realized
 479 using previously published data and web databases.

ID	I/UI @ D2	I/UI @ D10	Putative name
3.205	0,60	1,16	Choline
3.225	2,04	0,74	GPC
4.005	1,68	1,19	α -Fructose
4.015	1,75	1,17	β -Fructose
4.135	0,81	0,67	Proline
4.115	1,63	1,12	α -Fructose
3.215	1,81	0,82	GPC
3.055	0,84	1,00	Spermidine
1.775	0,85	0,98	Spermidine
1.765	0,87	1,02	Spermidine
3.045	0,84	0,99	Spermidine
5.235	1,15	1,05	α -Glucose
3.195	0,59	1,19	Choline
1.785	0,79	0,95	Spermidine
3.515	0,78	1,10	Choline
3.065	0,85	0,99	Spermidine
4.645	1,12	1,04	β -Glucose

480

481

482

483 References

- 484
485
486 Alaux, C., Brunet, J.-L., Dussaubat, C., Mondet, F., Tchamitchan, S., Cousin, M., Brillard, J., Baldy, A.,
487 Belzunces, L.P., Conte, Y.L., 2010a. Interactions between *Nosema* microspores and a
488 neonicotinoid weaken honeybees (*Apis mellifera*). *Environ. Microbiol.* 12, 774–782.
489 <https://doi.org/10.1111/j.1462-2920.2009.02123.x>
- 490 Alaux, C., Ducloz, F., Crauser, D., Le Conte, Y., 2010b. Diet effects on honeybee immunocompetence.
491 *Biol. Lett.* 6, 562–565. <https://doi.org/10.1098/rsbl.2009.0986>
- 492 Alaux, C., Folschweiller, M., McDonnell, C., Beslay, D., Cousin, M., Dussaubat, C., Brunet, J.-L., Conte,
493 Y.L., 2011. Pathological effects of the microsporidium *Nosema ceranae* on honey bee queen
494 physiology (*Apis mellifera*). *J. Invertebr. Pathol.* 106, 380–385.
495 <https://doi.org/10.1016/j.jip.2010.12.005>
- 496 Alaux, C., Sinha, S., Hasadsri, L., Hunt, G.J., Guzmán-Novoa, E., DeGrandi-Hoffman, G., Uribe-Rubio,
497 J.L., Southey, B.R., Rodriguez-Zas, S., Robinson, G.E., 2009. Honey bee aggression supports a
498 link between gene regulation and behavioral evolution. *Proc. Natl. Acad. Sci.* 106, 15400–
499 15405. <https://doi.org/10.1073/pnas.0907043106>
- 500 Aliferis, K.A., Copley, T., Jabaji, S., 2012. Gas chromatography–mass spectrometry metabolite
501 profiling of worker honey bee (*Apis mellifera* L.) hemolymph for the study of *Nosema*
502 *ceranae* infection. *J. Insect Physiol.* 58, 1349–1359.
503 <https://doi.org/10.1016/j.jinsphys.2012.07.010>
- 504 Alonso, A., Marsal, S., Julià, A., 2015. Analytical Methods in Untargeted Metabolomics: State of the
505 Art in 2015. *Front. Bioeng. Biotechnol.* 3. <https://doi.org/10.3389/fbioe.2015.00023>
- 506 Antúnez, K., Martín-Hernández, R., Prieto, L., Meana, A., Zunino, P., Higes, M., 2009. Immune
507 suppression in the honey bee (*Apis mellifera*) following infection by *Nosema ceranae*
508 (Microsporidia). *Environ. Microbiol.* 11, 2284–2290. <https://doi.org/10.1111/j.1462-2920.2009.01953.x>
- 510 Aufauvre, J., Biron, D.G., Vidau, C., Fontbonne, R., Roudel, M., Diogon, M., Viguès, B., Belzunces, L.P.,
511 Delbac, F., Blot, N., 2012. Parasite-insecticide interactions: a case study of *Nosema ceranae*
512 and fipronil synergy on honeybee. *Sci. Rep.* 2, 1–7. <https://doi.org/10.1038/srep00326>
- 513 Aufauvre, J., Misme-Aucouturier, B., Viguès, B., Texier, C., Delbac, F., Blot, N., 2014. Transcriptome
514 Analyses of the Honeybee Response to *Nosema ceranae* and Insecticides. *PLoS ONE* 9.
515 <https://doi.org/10.1371/journal.pone.0091686>
- 516 Bigliardi, E., Selmi, M.G., Lupetti, P., Corona, S., Gatti, S., Scaglia, M., Sacchi, L., 1996. Microsporidian
517 Spore Wall: Ultrastructural Findings on *Encephalitozoon hellem* Exospore. *J. Eukaryot.*
518 *Microbiol.* 43, 181–186. <https://doi.org/10.1111/j.1550-7408.1996.tb01388.x>
- 519 Boccard, J., Rudaz, S., 2014. Harnessing the complexity of metabolomic data with chemometrics. *J.*
520 *Chemom.* 28, 1–9. <https://doi.org/10.1002/cem.2567>
- 521 Bundy, J.G., Davey, M.P., Viant, M.R., 2008. Environmental metabolomics: a critical review and future
522 perspectives. *Metabolomics* 5, 3. <https://doi.org/10.1007/s11306-008-0152-0>
- 523 Chaimanee, V., Chantawannakul, P., Chen, Y., Evans, J.D., Pettis, J.S., 2012. Differential expression of
524 immune genes of adult honey bee (*Apis mellifera*) after inoculated by *Nosema ceranae*. *J.*
525 *Insect Physiol.* 58, 1090–1095. <https://doi.org/10.1016/j.jinsphys.2012.04.016>
- 526 Chaimanee, V., Warrit, N., Chantawannakul, P., 2010. Infections of *Nosema ceranae* in four different
527 honeybee species. *J. Invertebr. Pathol.* 105, 207–210.
528 <https://doi.org/10.1016/j.jip.2010.06.005>
- 529 Chen, Y.-W., Chung, W.-P., Wang, C.-H., Solter, L.F., Huang, W.-F., 2012. *Nosema ceranae* infection
530 intensity highly correlates with temperature. *J. Invertebr. Pathol.* 111, 264–267.
531 <https://doi.org/10.1016/j.jip.2012.08.014>

- Cox-Foster, D.L., Conlan, S., Holmes, E.C., Palacios, G., Evans, J.D., Moran, N.A., Quan, P.-L., Brieseman, T., Hornig, M., Geiser, D.M., Martinson, V., vanEngelsdorp, D., Kalkstein, A.L., Drysdale, A., Hui, J., Zhai, J., Cui, L., Hutchison, S.K., Simons, J.F., Egholm, M., Pettis, J.S., Lipkin, W.I., 2007. A Metagenomic Survey of Microbes in Honey Bee Colony Collapse Disorder. *Science* 318, 283–287. <https://doi.org/10.1126/science.1146498>
- Dussaubat, C., Brunet, J.-L., Higes, M., Colbourne, J.K., Lopez, J., Choi, J.-H., Martín-Hernández, R., Botías, C., Cousin, M., McDonnell, C., Bonnet, M., Belzunces, L.P., Moritz, R.F.A., Le Conte, Y., Alaux, C., 2012. Gut Pathology and Responses to the Microsporidium *Nosema ceranae* in the Honey Bee *Apis mellifera*. *PLoS ONE* 7. <https://doi.org/10.1371/journal.pone.0037017>
- Dussaubat, C., Maisonnasse, A., Alaux, C., Tchamitchan, S., Brunet, J.-L., Plettner, E., Belzunces, L.P., Le Conte, Y., 2010. *Nosema* spp. Infection Alters Pheromone Production in Honey Bees (*Apis mellifera*). *J. Chem. Ecol.* 36, 522–525. <https://doi.org/10.1007/s10886-010-9786-2>
- Dussaubat, C., Sagastume, S., Gómez-Moracho, T., Botías, C., García-Palencia, P., Martín-Hernández, R., Le Conte, Y., Higes, M., 2013. Comparative study of *Nosema ceranae* (Microsporidia) isolates from two different geographic origins. *Vet. Microbiol.* 162, 670–678. <https://doi.org/10.1016/j.vetmic.2012.09.012>
- Fan, T.W.-M., 1996. Metabolite profiling by one- and two-dimensional NMR analysis of complex mixtures. *Prog. Nucl. Magn. Reson. Spectrosc.* 28, 161–219. [https://doi.org/10.1016/0079-6565\(95\)01017-3](https://doi.org/10.1016/0079-6565(95)01017-3)
- Fiehn, O., 2002. Metabolomics--the link between genotypes and phenotypes. *Plant Mol. Biol.* 48, 155–171.
- Fleming, J.C., Schmehl, D.R., Ellis, J.D., 2015. Characterizing the Impact of Commercial Pollen Substitute Diets on the Level of *Nosema* spp. in Honey Bees (*Apis mellifera* L.). *PLOS ONE* 10, e0132014. <https://doi.org/10.1371/journal.pone.0132014>
- Franchet, A., Niehus, S., Caravello, G., Ferrandon, D., 2019. Phosphatidic acid as a limiting host metabolite for the proliferation of the microsporidium *Tubulosema ratisbonensis* in *Drosophila* flies. *Nat. Microbiol.* 4, 645–655. <https://doi.org/10.1038/s41564-018-0344-y>
- Fries, I., 2010. *Nosema ceranae* in European honey bees (*Apis mellifera*). *J. Invertebr. Pathol.* 103, S73–S79. <https://doi.org/10.1016/j.jip.2009.06.017>
- Giacomoni, F., Le Corguillé, G., Monsoor, M., Landi, M., Pericard, P., Pétéra, M., Duperier, C., Tremblay-Franco, M., Martin, J.-F., Jacob, D., Goulitquer, S., Thévenot, E.A., Caron, C., 2015. Workflow4Metabolomics: a collaborative research infrastructure for computational metabolomics. *Bioinformatics* 31, 1493–1495. <https://doi.org/10.1093/bioinformatics/btu813>
- Gisder, S., Hedtke, K., Möckel, N., Frielitz, M.-C., Linde, A., Genersch, E., 2010. Five-Year Cohort Study of *Nosema* spp. in Germany: Does Climate Shape Virulence and Assertiveness of *Nosema ceranae*? *Appl. Environ. Microbiol.* 76, 3032–3038. <https://doi.org/10.1128/AEM.03097-09>
- Goblirsch, M., Huang, Z.Y., Spivak, M., 2013. Physiological and Behavioral Changes in Honey Bees (*Apis mellifera*) Induced by *Nosema ceranae* Infection. *PLOS ONE* 8, e58165. <https://doi.org/10.1371/journal.pone.0058165>
- Goulson, D., Nicholls, E., Botías, C., Rotheray, E.L., 2015. Bee declines driven by combined stress from parasites, pesticides, and lack of flowers. *Science* 347. <https://doi.org/10.1126/science.1255957>
- Higes, M., Martín, R., Meana, A., 2006. *Nosema ceranae*, a new microsporidian parasite in honeybees in Europe. *J. Invertebr. Pathol.* 92, 93–95. <https://doi.org/10.1016/j.jip.2006.02.005>
- Higes, M., Meana, A., Bartolomé, C., Botías, C., Martín-Hernández, R., 2013. *Nosema ceranae* (Microsporidia), a controversial 21st century honey bee pathogen. *Environ. Microbiol. Rep.* 5, 17–29. <https://doi.org/10.1111/1758-2229.12024>
- Holt, H.L., Aronstein, K.A., Grozinger, C.M., 2013. Chronic parasitization by *Nosema* microsporidia causes global expression changes in core nutritional, metabolic and behavioral pathways in honey bee workers (*Apis mellifera*). *BMC Genomics* 14, 799. <https://doi.org/10.1186/1471-2164-14-799>

- Invernizzi, C., Abud, C., Tomasco, I.H., Harriet, J., Ramallo, G., Campá, J., Katz, H., Gardiol, G.,
Mendoza, Y., 2009. Presence of *Nosema ceranae* in honeybees (*Apis mellifera*) in Uruguay. *J.*
Invertebr. Pathol. 101, 150–153. <https://doi.org/10.1016/j.jip.2009.03.006>
- Kelkenberg, M., Odman-Naresh, J., Muthukrishnan, S., Merzendorfer, H., 2015. Chitin is a necessary
component to maintain the barrier function of the peritrophic matrix in the insect midgut.
Insect Biochem. Mol. Biol. 56, 21–28. <https://doi.org/10.1016/j.ibmb.2014.11.005>
- Kuhl, C., Tautenhahn, R., Böttcher, C., Larson, T.R., Neumann, S., 2012. CAMERA: An integrated
strategy for compound spectra extraction and annotation of LC/MS data sets. *Anal. Chem.*
84, 283. <https://doi.org/10.1021/ac202450g>
- Kurze, C., Conte, Y.L., Dussaubat, C., Erler, S., Kryger, P., Lewkowski, O., Müller, T., Widder, M.,
Moritz, R.F.A., 2015. *Nosema* Tolerant Honeybees (*Apis mellifera*) Escape Parasitic
Manipulation of Apoptosis. *PLOS ONE* 10, e0140174.
<https://doi.org/10.1371/journal.pone.0140174>
- Lankadurai, B.P., Nagato, E.G., Simpson, M.J., 2013. Environmental metabolomics: an emerging
approach to study organism responses to environmental stressors. *Environ. Rev.* 21, 180–
205. <https://doi.org/10.1139/er-2013-0011>
- Li, W., Chen, Y., Cook, S.C., 2018. Chronic *Nosema ceranae* infection inflicts comprehensive and
persistent immunosuppression and accelerated lipid loss in host *Apis mellifera* honey bees.
Int. J. Parasitol. 48, 433–444. <https://doi.org/10.1016/j.ijpara.2017.11.004>
- Liu, X., Locasale, J.W., 2017. Metabolomics: A Primer. *Trends Biochem. Sci.* 42, 274–284.
<https://doi.org/10.1016/j.tibs.2017.01.004>
- Martín-Hernández, R., Botías, C., Barrios, L., Martínez-Salvador, A., Meana, A., Mayack, C., Higes, M.,
2011. Comparison of the energetic stress associated with experimental *Nosema ceranae* and
Nosema apis infection of honeybees (*Apis mellifera*). *Parasitol. Res.* 109, 605–612.
<https://doi.org/10.1007/s00436-011-2292-9>
- Mayack, C., Naug, D., 2010. Parasitic infection leads to decline in hemolymph sugar levels in
honeybee foragers. *J. Insect Physiol.* 56, 1572–1575.
<https://doi.org/10.1016/j.jinsphys.2010.05.016>
- Mayack, C., Naug, D., 2009. Energetic stress in the honeybee *Apis mellifera* from *Nosema ceranae*
infection. *J. Invertebr. Pathol.* 100, 185–188. <https://doi.org/10.1016/j.jip.2008.12.001>
- Medici, S.K., Sarlo, E.G., Porrini, M.P., Braunstein, M., Eguaras, M.J., 2012. Genetic variation and
widespread dispersal of *Nosema ceranae* in *Apis mellifera* apiaries from Argentina. *Parasitol.*
Res. 110, 859–864. <https://doi.org/10.1007/s00436-011-2566-2>
- Monnerie, S., Petera, M., Lyan, B., Gaudreau, P., Comte, B., Pujos-Guillot, E., 2019. Analytic
Correlation Filtration: A New Tool to Reduce Analytical Complexity of Metabolomic Datasets.
Metabolites 9. <https://doi.org/10.3390/metabo9110250>
- Naug, D., Gibbs, A., 2009. Behavioral changes mediated by hunger in honeybees infected with
Nosema ceranae. *Apidologie* 40, 595–599. <https://doi.org/10.1051/apido/2009039>
- Nicholson, J.K., Foxall, P.J.D., Spraul, Manfred., Farrant, R.Duncan., Lindon, J.C., 1995. 750 MHz ¹H
and ¹H-¹³C NMR Spectroscopy of Human Blood Plasma. *Anal. Chem.* 67, 793–811.
<https://doi.org/10.1021/ac00101a004>
- Paris, L., El Alaoui, H., Delbac, F., Diogon, M., 2018. Effects of the gut parasite *Nosema ceranae* on
honey bee physiology and behavior. *Curr. Opin. Insect Sci., Ecology •*
Parasites/Parasitoids/Biological control 26, 149–154.
<https://doi.org/10.1016/j.cois.2018.02.017>
- Pettis, J.S., vanEngelsdorp, D., Johnson, J., Dively, G., 2012. Pesticide exposure in honey bees results
in increased levels of the gut pathogen *Nosema*. *Naturwissenschaften* 99, 153–158.
<https://doi.org/10.1007/s00114-011-0881-1>
- Retschnig, G., Neumann, P., Williams, G.R., 2014. Thiadiazole–*Nosema ceranae* interactions in honey
bees: Host survivorship but not parasite reproduction is dependent on pesticide dose. *J.*
Invertebr. Pathol. 118, 18–19. <https://doi.org/10.1016/j.jip.2014.02.008>

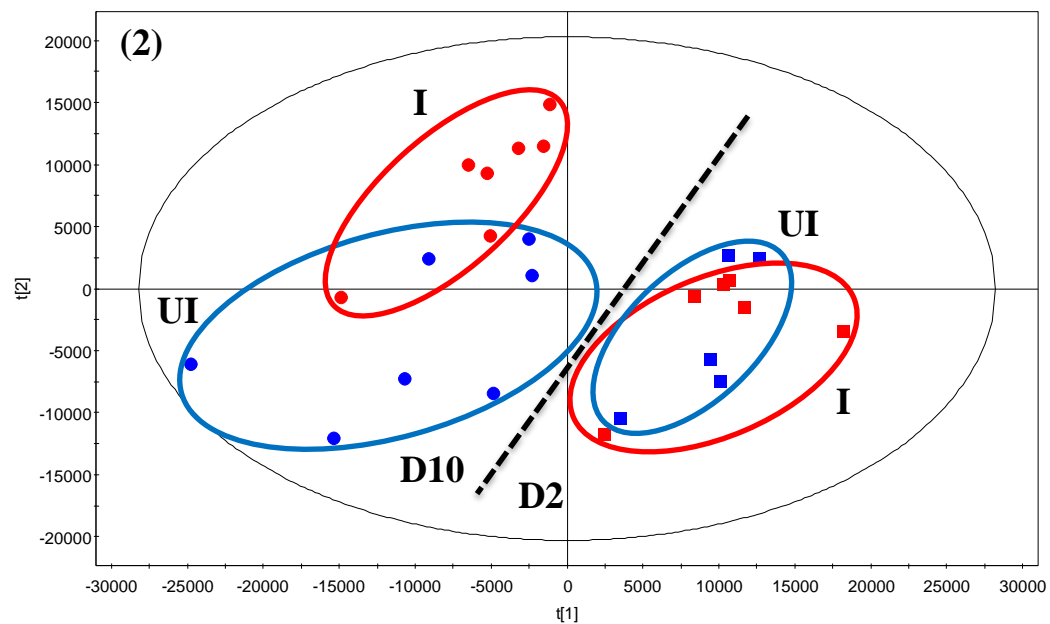
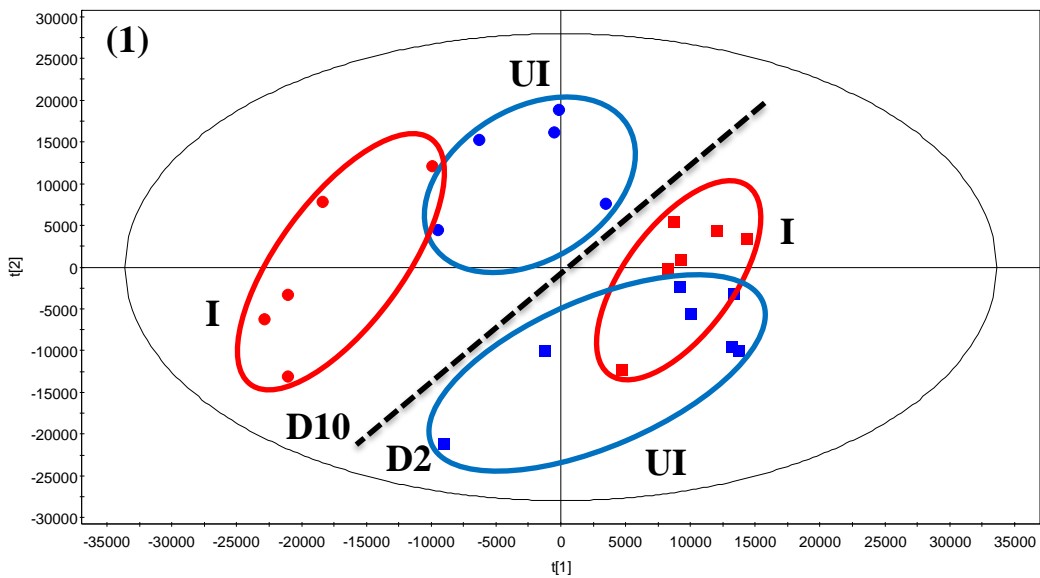
- Simón-Manso, Y., Lowenthal, M.S., Kilpatrick, L.E., Sampson, M.L., Telu, K.H., Rudnick, P.A., Mallard, W.G., Bearden, D.W., Schock, T.B., Tchekhovskoi, D.V., Blonder, N., Yan, X., Liang, Y., Zheng, Y., Wallace, W.E., Neta, P., Phinney, K.W., Remaley, A.T., Stein, S.E., 2013. Metabolite Profiling of a NIST Standard Reference Material for Human Plasma (SRM 1950): GC-MS, LC-MS, NMR, and Clinical Laboratory Analyses, Libraries, and Web-Based Resources. *Anal. Chem.* 85, 11725–11731. <https://doi.org/10.1021/ac402503m>
- The Metabolomics Standards Initiative (MSI) and Core Information for Metabolomics Reporting (CIMR) [WWW Document], n.d. URL msi.html (accessed 3.10.20).
- vanEngelsdorp, D., Evans, J.D., Saegerman, C., Mullin, C., Haubruge, E., Nguyen, B.K., Frazier, M., Frazier, J., Cox-Foster, D., Chen, Y., Underwood, R., Tarpy, D.R., Pettis, J.S., 2009. Colony Collapse Disorder: A Descriptive Study. *PLOS ONE* 4, e6481. <https://doi.org/10.1371/journal.pone.0006481>
- vanEngelsdorp, D., Meixner, M.D., 2010. A historical review of managed honey bee populations in Europe and the United States and the factors that may affect them. *J. Invertebr. Pathol.* 103, S80–S95. <https://doi.org/10.1016/j.jip.2009.06.011>
- Vidau, C., Diogon, M., Aufauvre, J., Fontbonne, R., Viguès, B., Brunet, J.-L., Texier, C., Biron, D.G., Blot, N., El Alaoui, H., Belzunces, L.P., Delbac, F., 2011. Exposure to Sublethal Doses of Fipronil and Thiacloprid Highly Increases Mortality of Honeybees Previously Infected by *Nosema ceranae*. *PLoS ONE* 6. <https://doi.org/10.1371/journal.pone.0021550>
- Wang, L., Meeus, I., Rombouts, C., Meulebroek, L.V., Vanhaecke, L., Smagghe, G., 2019. Metabolomics-based biomarker discovery for bee health monitoring: A proof of concept study concerning nutritional stress in *Bombus terrestris*. *Sci. Rep.* 9, 1–11. <https://doi.org/10.1038/s41598-019-47896-w>
- Williams, G.R., Sampson, M.A., Shutler, D., Rogers, R.E.L., 2008. Does fumagillin control the recently detected invasive parasite *Nosema ceranae* in western honey bees (*Apis mellifera*)? *J. Invertebr. Pathol.* 99, 342–344. <https://doi.org/10.1016/j.jip.2008.04.005>
- Willker, W., Engelmann, J., Brand, A., Liedfritz, D., 1996. Metabolite Identification in Cell Extracts and Culture Media by Proton-detected D-H, C-NMR Spectroscopy1. *J. Magn. Reson. Anal.* 21–32.
- Wishart, D.S., Lewis, M.J., Morrissey, J.A., Flegel, M.D., Jeroncic, K., Xiong, Y., Cheng, D., Eisner, R., Gautam, B., Tzur, D., Sawhney, S., Bamforth, F., Greiner, R., Li, L., 2008. The human cerebrospinal fluid metabolome. *J. Chromatogr. B Analyt. Technol. Biomed. Life. Sci.* 871, 164–173. <https://doi.org/10.1016/j.jchromb.2008.05.001>
- Wu, J.Y., Smart, M.D., Anelli, C.M., Sheppard, W.S., 2012. Honey bees (*Apis mellifera*) reared in brood combs containing high levels of pesticide residues exhibit increased susceptibility to *Nosema* (Microsporidia) infection. *J. Invertebr. Pathol.* 109, 326–329. <https://doi.org/10.1016/j.jip.2012.01.005>
- Zhang, A., Sun, H., Wu, X., Wang, X., 2012. Urine metabolomics. *Clin. Chim. Acta* 414, 65–69. <https://doi.org/10.1016/j.cca.2012.08.016>
- Zhang, X., Li, Q., Xu, Z., Dou, J., 2020. Mass spectrometry-based metabolomics in health and medical science: a systematic review. *RSC Adv.* 10, 3092–3104. <https://doi.org/10.1039/C9RA08985C>
- Zhao, X., Fritsche, J., Wang, J., Chen, J., Rittig, K., Schmitt-Kopplin, P., Fritsche, A., Häring, H.-U., Schleicher, E.D., Xu, G., Lehmann, R., 2010. Metabonomic fingerprints of fasting plasma and spot urine reveal human pre-diabetic metabolic traits. *Metabolomics* 6, 362–374. <https://doi.org/10.1007/s11306-010-0203-1>

Web references

- « Human Metabolome Database ». <https://hmdb.ca/>.
- « KEGG: Kyoto Encyclopedia of Genes and Genomes ». <https://www.genome.jp/kegg/>.
- « MassBank | MSSJ MassBank Mass Spectral DataBase ». <http://www.massbank.jp/>.

684 « PRIME: Platform for RIKEN Metabolomics ».
685 http://prime.psc.riken.jp/?action=standard_index.

Fig.1: PLS-DA on LC/MS profiles.



R2X[1] = 0,209422

R2X[2] = 0,124118

Ellipse: Hotelling T2 (0,95)

SIMCA-P+ 12.0.1 - 2019-11-06 16:52:52 (UTC+1)

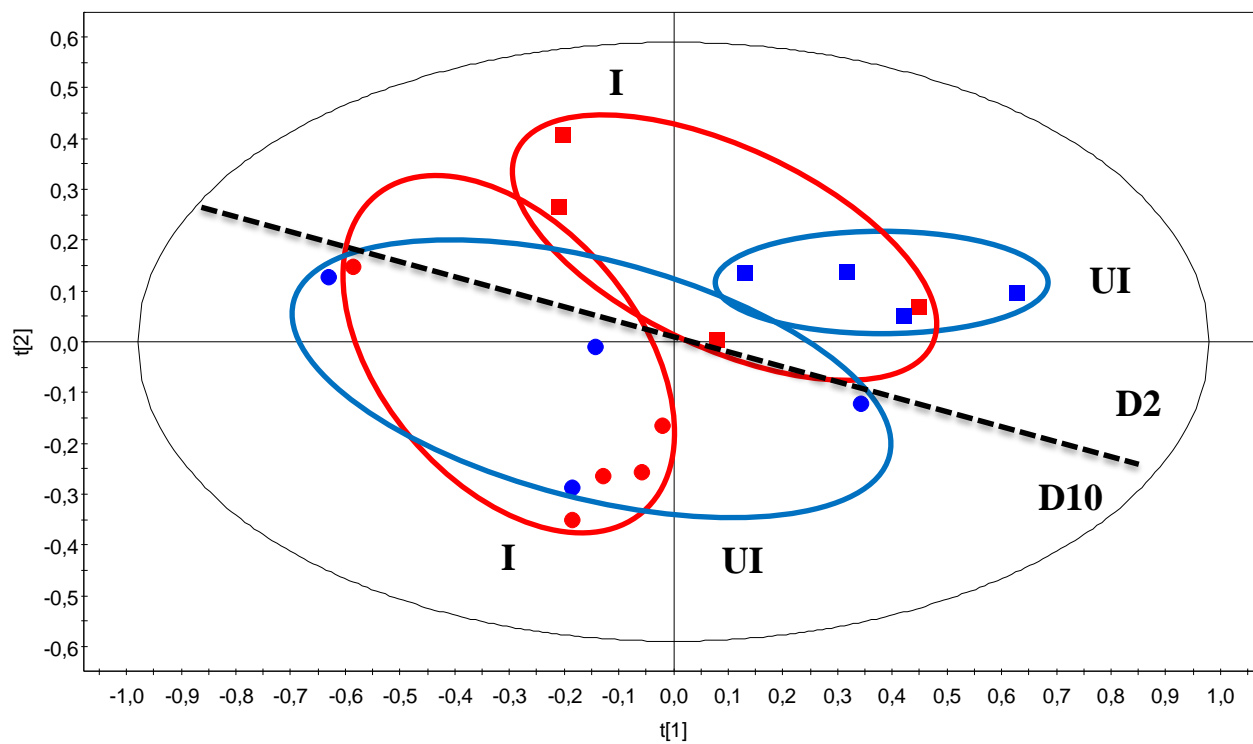


Fig.2: PLS-DA on NMR data.

